

# Deformation behavior and microstructure evolution in multistage hot working of TA15 titanium alloy: on the role of recrystallization

X. G. Fan · H. Yang · P. F. Gao

Received: 10 November 2010 / Accepted: 16 April 2011 / Published online: 30 April 2011  
© Springer Science+Business Media, LLC 2011

**Abstract** Interrupted compression tests of TA15 titanium alloy with initially equiaxed microstructure were carried out at deformation temperatures between 1173 to 1273 K and strain rates between 0.001 to 0.1 s<sup>-1</sup> to investigate the deformation behavior and microstructure evolution under multistage deformation. The TA15 alloy exhibits significant flow softening in both  $\beta$  and ( $\alpha + \beta$ ) working. It is found that the flow softening relates to dynamic recrystallization of  $\beta$  phases under current experimental conditions. In multistage  $\beta$  working, metadynamic recrystallization is the main softening mechanism during inter-pass holding. The grain refinement by metadynamic recrystallization leads to the decrease in peak stress upon reloading. In multistage ( $\alpha + \beta$ ) working, static recrystallization is the main softening mechanism during inter-pass holding. The static recrystallization kinetics increases with temperature and strain rate. The inter-pass holding has little influence on the morphology of the primary  $\alpha$  phases. The  $\beta$  grain size is determined by spacing of primary  $\alpha$  phases, which is more affected by working temperature but less dependent on strain rate and inter-pass holding time.

**Keywords** Multistage deformation · TA15 titanium alloy · Flow stress · Microstructure · Recrystallization

## Introduction

TA15 (Ti–6Al–2Zr–1Mo–1V) is a near- $\alpha$  titanium alloy of moderate room-temperature and high-temperature strength, good thermal stability, and welding performance which is widely used to manufacture structural components in aeroplanes. Thermo-mechanical processing of TA15 alloy is performed in the ( $\alpha + \beta$ ) phase field and single  $\beta$  phase field to obtain the required microstructure and properties. As a two phase titanium alloy, the TA15 titanium alloy is well known for the narrow processing window and high deformation resistance during hot working. Therefore, the TA15 billet often goes through numerous operations, including successive multi-pass deformation and reheating to achieve the final product. In multi-step thermo-mechanical processing of metals and alloys, diverse microstructure changes may take place, such as recovery (static and dynamic), recrystallization (static, dynamic and metadynamic), and grain growth. Furthermore, the allotropic  $\alpha/\beta$  phase transformation of two phase titanium alloys complicates the microstructure evolution and produces a wide variation in the scale and morphology of phases [1]. The above microstructure changes are mainly determined by the thermo-mechanical processing. Meanwhile, they also have great influence on the hot working behavior during processing as well as the mechanical properties after deformation, and thus affect the forming process. Consequently, understanding the interaction between multistage thermo-mechanical processing and microstructure evolution is critical to the development of high forming quality and attractive service performance.

By now, some research has been carried out on the deformation behavior and microstructure evolution of TA15 alloy in single-hit deformation. Liu et al. [2] investigated the hot compressive behavior and microstructure evolution of TA15 alloy with initially equiaxed

---

X. G. Fan (✉) · H. Yang · P. F. Gao  
State Key Laboratory of Solidification Processing, School of Materials Science and Engineering, Northwestern Polytechnical University, P.O. Box 542, Xi'an 710072, People's Republic of China  
e-mail: fxg3200@126.com

microstructure at 1073 K. It is found that the flow stress decreases with strain to a stable stage after the peak stress and the grain size decreases at first and then increases. TEM observation confirmed that dynamic recrystallization (DRX) of the primary equiaxed  $\alpha$  phases account for such phenomena. Sun et al. [3] also suggested that DRX of the primary  $\alpha$  plays an important role in subtransus forging of TA15 alloy. However, the multistage deformation still needs further investigation.

For materials undergoing DRX, the post-deformation static recrystallization (SRX) and metadynamic recrystallization (MDRX) can change the deformation behavior in the subsequent deformation and influence the final microstructure. Therefore, together with DRX, they have received considerable interest in many metals, such as steels [4, 5], nickel-based alloys [6], magnesium alloys [7] and titanium alloys [1]. During  $\beta$  working of two phase titanium alloys, SRX dominates the grain refinement due to the high level of recovery associated with the high stacking fault energy of body-centered cubic (bcc)  $\beta$  crystal structure [8], though a small fraction of DRX has been reported for Ti–6Al–4V [9], IMI834 [1], and Ti–1100 alloy [10]. In subtransus deformation, DRX of both  $\alpha$  and  $\beta$  has been observed. Vo et al. [1] found that dynamic and static  $\beta$  recrystallization take place in hot working of near- $\alpha$  IMI834 alloy with initially bimodal microstructure while  $\alpha$  recrystallization is not observed.  $\beta$  recrystallization is accelerated with decreasing temperature which is quite different from the  $\beta$  working. Similar behavior has been reported for near- $\alpha$  Ti–1100 alloy by Ma et al. [10]. Jackson et al. [11] reported that the dominant restoration mechanism of Ti–10V–2Fe–3Al changes from dynamic recovery (DRV) to DRX with decreasing temperature. Zong et al. [12] found that only  $\alpha$  recrystallization takes place in hot deformation of TC11 alloy and the recrystallized grain size is not affected by the hot working parameters. Zong et al. [13] reported that both  $\alpha$  phases and  $\beta$  phases undergo DRX in hot working of a Ti–4.5Al–3Mo–1V alloy and DRX occurs more rapidly in  $\alpha$  phases than in  $\beta$  phases. However, the effect of recrystallization on the deformation behavior and microstructure of TA15 alloy needs to be systematically investigated.

In this study, the deformation behavior and microstructure evolution of TA15 alloy were investigated through interrupted compression tests combined with metallographic observation. The results provide basis for process design and microstructure control in thermo-mechanical processing of near- $\alpha$  titanium alloys.

## Experimental procedures

The TA15 titanium alloy, with chemical composition (wt%) of 6.06 Al, 2.08 Mo, 1.32 V, 1.86 Zr, 0.30 Fe, and Ti

in balance, was supplied in the form of 80 mm thick by 170 mm wide hot rolled plate which had been annealed at 1123 K for 2 h and air cooled. The measured  $\beta$ -transus temperature was 1263 K. The microstructure of as-received material consisted of  $\sim 60\%$  equiaxed primary  $\alpha$  phases within transformed  $\beta$  matrix, as shown in Fig. 1. Equiaxed  $\alpha$  grains were pancaked slightly along the normal direction. The average thickness and aspect ratio of the elongated  $\alpha$  grains are about 5.7 and 2.4  $\mu\text{m}$ , respectively. Cylindrical specimens of 15 mm in height and 10 mm in diameter were machined from the plate, of which the axis was parallel to the normal direction of the as-received bar.

To study the multistage deformation behavior, isothermal interrupted compression tests were conducted on a Gleeble-3500 thermal simulator. A thin graphite layer was placed between the specimen and die to minimize friction. The specimens were heated to the deformation temperature at a rate of 10 K/s, held for 3 min to impart thermal equilibration. The interrupted compression tests were performed at temperatures of 1173–1273 K, strain rates of 0.001–0.1  $\text{s}^{-1}$  up to a total strain of 0.9. The deformation was interrupted at a strain of 0.45. During the interruption, the specimens were held at the deformation temperature for 0–600 s. After the second deformation, the specimens were water quenched. Corresponding single-hit compression tests were also carried out for comparison.

After the compression tests, the specimens were sectioned along the compression axis, mechanically grinded and polished, and etched with a solution of 13% $\text{HNO}_3$ , 7% $\text{HF}$ , and 80% $\text{H}_2\text{O}$ . Microstructural examination was performed on a LECIA DFC320 microscope.

## Results and discussion

### Microstructure prior to deformation

Figure 2 illustrates the microstructures of the alloy annealed at different temperatures. In the ( $\alpha + \beta$ ) phase field, the volume fraction of primary  $\alpha$  ( $\alpha_p$ ) decreases with temperature. The measured  $\alpha_p$  percentage as a function of annealing temperature is given in Fig. 3. The primary  $\alpha$  grain size decreases slightly with temperature because of phase transformation. The lamellar  $\alpha$  phases are not fully transformed into  $\beta$  phases below 1193 K (Fig. 2a). The retained lamellar  $\alpha$  are about 1.2  $\mu\text{m}$  thick, and they are gradually transformed into  $\beta$  phases with increasing temperature (Fig. 2b). The growth of  $\beta$  grains are greatly restrained by primary  $\alpha$  phases below the  $\beta$  transus temperature (about 9.5 and 11.7  $\mu\text{m}$  at 1213 and 1233 K). In the  $\beta$  phase field, grain growth increases the  $\beta$  grain size to about 220  $\mu\text{m}$  at 1273 K due to the rapid self-diffusion of  $\beta$  phase (Fig. 2c).

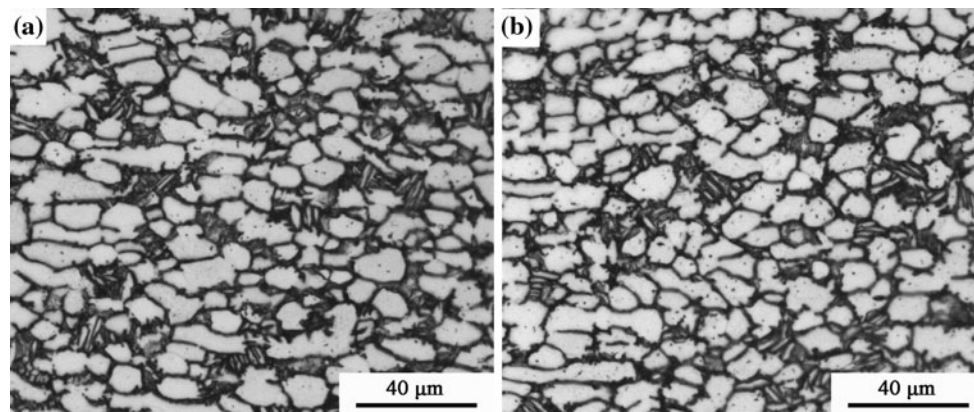


**Fig. 1** Microstructure of as-received material at **a** rolling plane and **b** transverse plane

### Stress–strain curves and microstructure of the single-hit deformation

Typical uninterrupted stress–strain curves of TA15 titanium alloy are given in Fig. 4. The uninterrupted curves exhibit low peak strain followed by flow softening under the experimental conditions. Similar phenomenon has been reported for near- $\alpha$  IMI834 alloy [1, 14], and two phase Ti–6.5Al–3.5Mo–1.5Zr–0.3Si alloy [15].

The softening mechanisms of two phase titanium alloys vary with hot working conditions as well as initial microstructure. In the  $\beta$  phase field, it is widely accepted that DRV is the main softening mechanism due to the high stacking fault energy and rapid self diffusion of the bcc  $\beta$  phase [16]. As a result, flow softening is not significant. However, a small amount of DRX may take place at large strain. Vo et al. [1] found that the volume fraction of DRX was less than 15% up to a strain of 1 in  $\beta$  working of IMI834 alloy and the variation of temperature and strain rate produces minor changes in the level of DRX. Ding et al. [17] reported a maximum recrystallization percentage of 29.8% at 1050°C and  $1.0 \text{ s}^{-1}$  during  $\beta$  working of Ti–6Al–4V alloy. It is also found that recrystallization kinetics increases with strain rate [1, 17], which is different from the materials with low-to-medium stacking fault energy [18]. This is because high strain rate decreases the level of DRV. In the current study, DRX also occurs in the  $\beta$  phase field, as shown in Fig. 5. Figure 5 illustrates the microstructures at different strain rates. The microstructure mainly consisted of equiaxed grains at a strain rate of  $0.01 \text{ s}^{-1}$ , indicating a high level of DRX. However, pancaked prior  $\beta$  grains were observed with a necklace of small equiaxed grains at the grain boundaries at a strain rate of  $10 \text{ s}^{-1}$ , which suggests that only a small amount of DRX took place. Therefore, the recrystallization kinetics decreases with strain rate. The strain rate has strong influence on recrystallization rate. These phenomena are

different from the IMI834 alloy and Ti–6Al–4V alloy. Besides, the DRX percentage is much larger than that of the IMI834 alloy and Ti–6Al–4V alloy. In this study, DRX may also attribute to the flow stress drop in  $\beta$  working.

When the titanium alloy with an initially equiaxed microstructure is deformed in the  $\alpha + \beta$  phase field, flow softening may be induced by recrystallization ( $\alpha$  recrystallization,  $\beta$  recrystallization, or both of them) and flow localization. The flow localization, which is caused by adiabatic heating, generally takes place at low temperature and high strain rate. It has not been observed under current experimental conditions and can not account for the softening in this investigation. The large stress drop suggests that recrystallization plays an important role in ( $\alpha + \beta$ ) working. The microstructure after deformation in the ( $\alpha + \beta$ ) phase field is shown in Fig. 6. In the upper ( $\alpha + \beta$ ) phase field (Fig. 6b), the  $\alpha_p$  grains were elongated transverse to the compression axis. The  $\alpha_p$  grain boundaries were smooth, indicating the absence of DRX in  $\alpha_p$  grains. Both pancaked and equiaxed  $\beta$  grains were observed. The results show that  $\beta$  recrystallization took place. In the lower ( $\alpha + \beta$ ) phase field (Fig. 6a), the  $\alpha_p$  grain boundaries were wavy as the strain imposed on  $\alpha_p$  increased with decreasing temperature. However, no evidence of  $\alpha_p$  recrystallization was observed. The residual lamellar  $\alpha$  were broken up, resulting in some fine equiaxed  $\alpha$  phases. However, the volume fraction of fine equiaxed  $\alpha$  is minor. Small equiaxed  $\beta$  grains were found among the  $\alpha_p$  grains. Therefore,  $\beta$  recrystallization is the main softening mechanism.

Liu et al. [2] reported  $\alpha$  recrystallization during deformation of TA15 alloy at 1073 K. The temperature employed in their investigation was much lower than this study at which  $\alpha$  phases were dominant (about 175 K below  $\beta$  transus). The  $\alpha_p$  are harder than  $\beta$  matrix, so the  $\alpha_p$  undergo less deformation than  $\beta$  matrix. Self consistent analysis of wrought two phase alloys [19, 20] revealed that

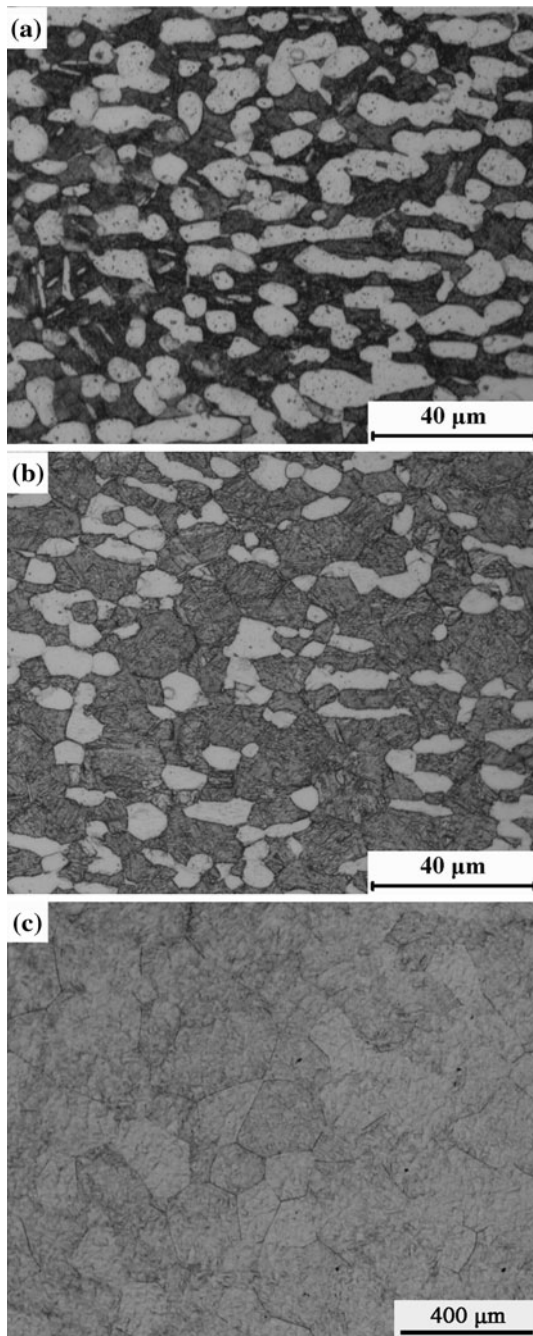


**Fig. 2** Microstructure prior to deformation at **a** 1193 K, **b** 1233 K, and **c** 1273 K

the strain partitioning between  $\alpha_p$  and  $\beta$  matrix increases with temperature. Under the experimental conditions of Liu et al. [2],  $\alpha_p$  undergo most of the deformation and there was enough stored energy for the nucleation and growth of recrystallizing grains. In this study, however, the strain imposed on  $\alpha_p$  was much smaller than that on  $\beta$  matrix. The  $\alpha$  recrystallization was suppressed. Meanwhile, the existence of harder  $\alpha_p$  would increase the deformation

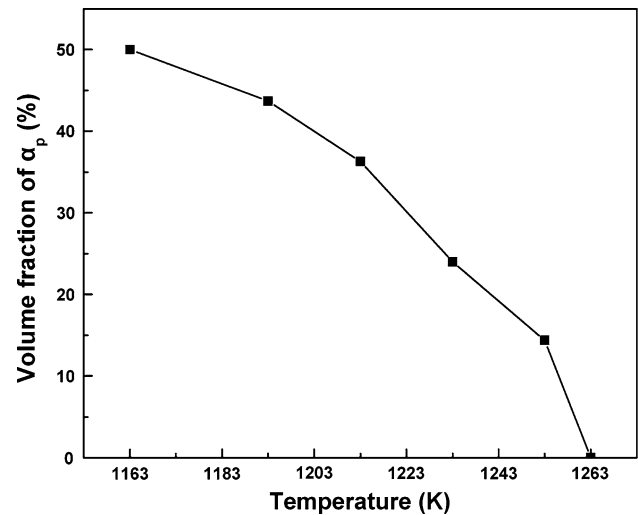


**Fig. 3** Effect of temperature on the volume fraction of  $\alpha_p$

inhomogeneity and provide more nuclei for recrystallization [1]. As a result,  $\beta$  recrystallization was accelerated.

An empirical method to depict the dependence of flow stress on temperature and strain rate in hot working is given by:

$$\dot{\epsilon} = A\sigma^{1/m} \exp\left(-\frac{Q}{RT}\right) \quad (1)$$

where  $\dot{\epsilon}$  is the strain rate ( $s^{-1}$ ),  $Q$  the apparent activation energy for deformation ( $kJ\ mol^{-1}$ ),  $\sigma$  the flow stress (MPa),  $T$  the absolute deformation temperature (K),  $m$  the strain rate sensitivity parameter,  $R$  the gas constant ( $8.3145\ J\ mol^{-1}\ K^{-1}$ ) and  $A$  the material constant. From Eq. 1,  $Q$  can be calculated by:

$$Q = -\frac{R}{m} \left. \frac{\partial \ln \sigma}{\partial (1/T)} \right|_{\dot{\epsilon}} \quad (2)$$

The variation of flow stress with temperature and strain rate is plotted in Fig. 7. Calculated apparent activation energies in  $\beta$  and  $(\alpha + \beta)$  phase fields are 219 and 760  $kJ\ mol^{-1}$ . The apparent activation energy in  $(\alpha + \beta)$  phase field is much higher than the reported activation energy for diffusion in  $\alpha$  phase ( $150\ kJ\ mol^{-1}$ ) and  $\beta$  phase ( $153\ kJ\ mol^{-1}$ ) [20], which is consistent with previous studies on a wide range of two phase titanium alloys [14, 21–24]. However, the high apparent activation energy may be caused by the dependence of flow stress and volume fraction of different phases on temperature, and can not be directly related to the deformation mechanism in two phase materials [25]. The apparent activation energy in  $\beta$  phase field is a little higher than the activation energy for diffusion in  $\beta$  phase, which indicates that DRX may play an important role during  $\beta$  working.

**Fig. 4** Uninterrupted stress–strain curves under different hot working conditions

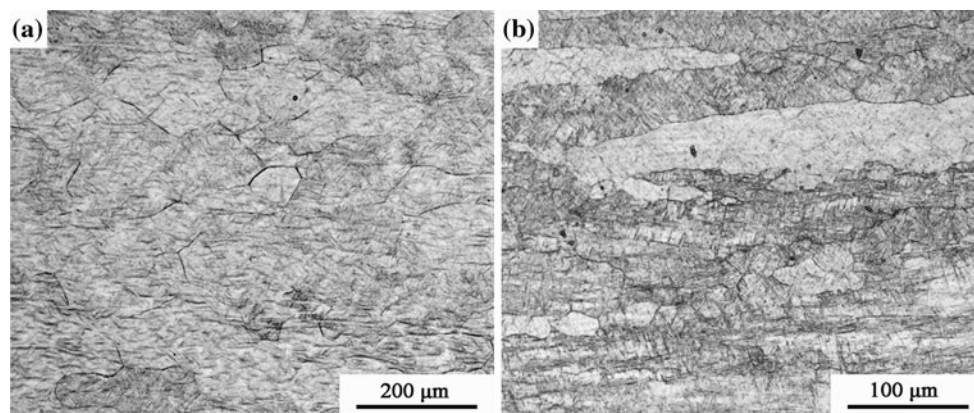
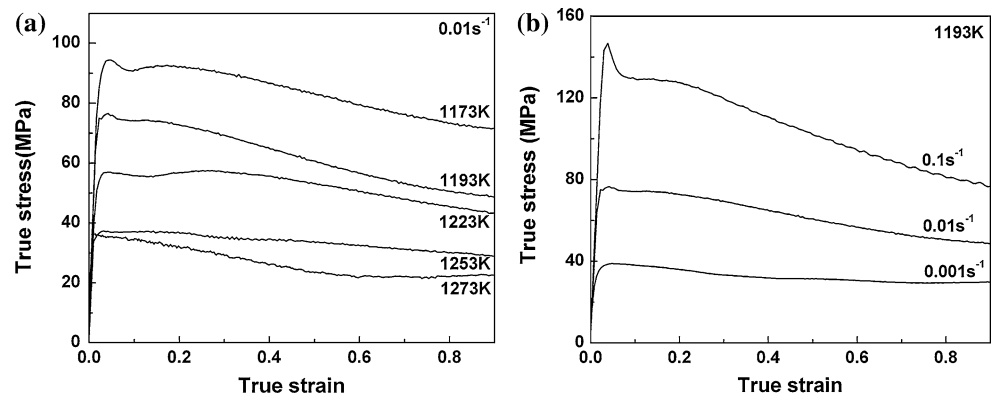


**Fig. 5** Microstructure after deformation at a temperature of 1273 K, strain of 0.9 and different strain rates: **a**  $0.01 \text{ s}^{-1}$  and **b**  $10 \text{ s}^{-1}$

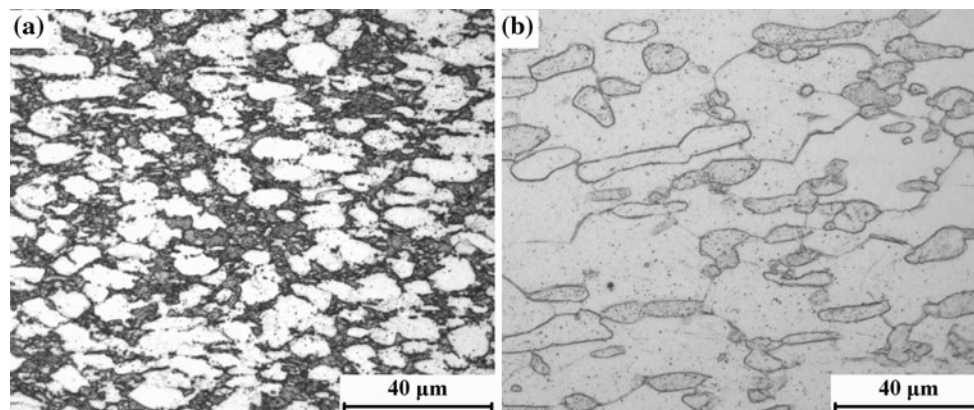


**Fig. 6** Microstructure after deformation at a strain rate of  $0.01 \text{ s}^{-1}$ , strain of 0.9 and temperatures of **a** 1173 K and **b** 1243 K

Multistage deformation behavior and microstructure evolution

#### *Multistage $\beta$ working*

For multistage deformation process, the restoration processes, e.g., recovery and recrystallization occur during interruption, which reduce the stored energy of deformation, reconstruct the microstructure and thereby influence

the plastic deformation behavior as well as microstructure in the following deformation.

Figure 8 illustrates the typical interrupted stress–strain curve in the  $\beta$  phase field. The deformation was interrupted at a strain of 0.45, which was much larger than the peak strain. The interruption time ( $t_{\text{int}}$ ) adopted in the test was 100 s, which is comparable to the deformation time. The flow stress curves have been normalized to the average stress prior to interruption.

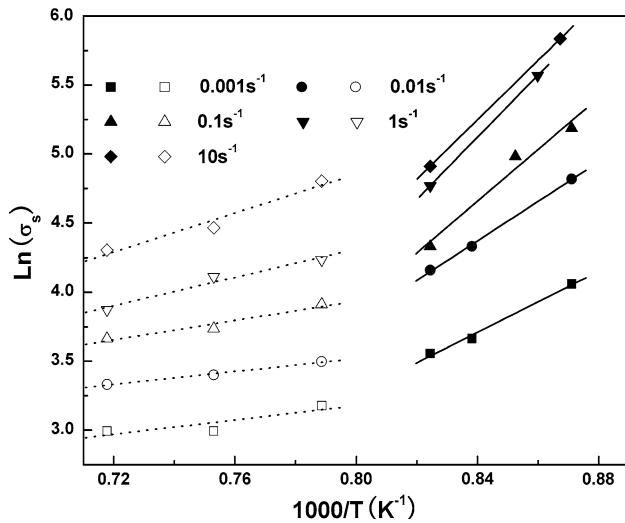


**Fig. 7** Variation of flow stress with temperature in two phase field and  $\beta$  phase field

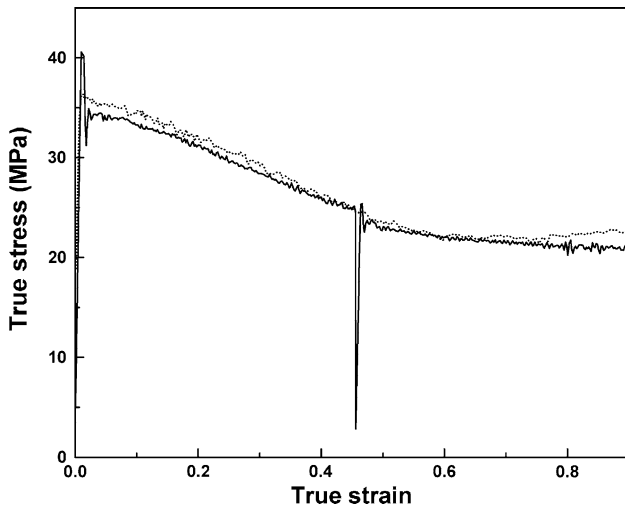


**Fig. 8** Interrupted stress–strain curve at  $T = 1273$  K,  $\dot{\epsilon} = 0.01$  s $^{-1}$ ,  $t_{int} = 100$  s. The uninterrupted stress–strain curve is given in *dot form*

In the second deformation, the discontinuous yield drop reappeared. This was followed by a slight working hardening and flow softening. Then the flow stress converged to a steady state. The steady state flow stress was close to that in the single-hit deformation. However, the peak stress was much smaller than that of the first deformation and close to the flow stress prior to interruption.

The discontinuous yield phenomenon has been ascribed to a sudden mobile dislocation generation from grain boundaries [26]. Therefore, the reappearance of discontinuous yielding is often associated with fully reconstructed microstructure [1]. This is confirmed by metallurgical observation. Figure 9a illustrates the microstructure at the interruption strain without holding. Both large pancaked prior  $\beta$  grains and small equiaxed recrystallizing  $\beta$  grains were observed, indicating a partly recrystallized microstructure. After isothermal holding at the deformation temperature, a fully equiaxed microstructure was easily achieved, as shown in Fig. 9b. Therefore, MDRX occurred during the interruption, as an incubation time is needed for nucleation of SRX which retards the softening process in the beginning. Vo et al. [1] found that the softening fraction increased by only 10% after 100 s holding during  $\beta$  working of IMI834 alloy at 0.01 s $^{-1}$ , which is much smaller than this study.

The peak value and softening fraction of flow stress in the second deformation were smaller than that in the first deformation, which may be due to grain refinement after the first deformation (Fig. 9b, 2c). For materials undergoing DRX, the initial grain size has a significant influence on the flow stress behavior. A fine grained structure provides more nucleation sites for recrystallization, which accelerates the recrystallization and consequently reduces the peak stress and the flow softening [27]. The microstructure was refined prior to the second deformation (Fig. 9b). Therefore, the peak stress and flow softening decreased. The microstructure after the second deformation showed a large

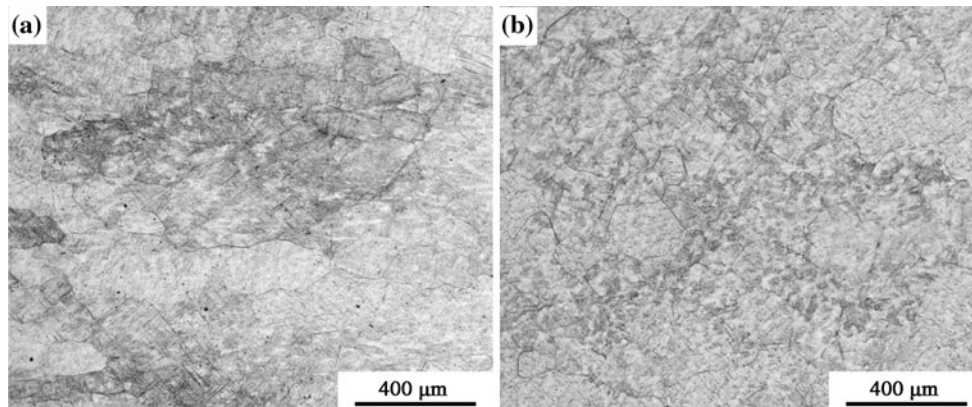


**Fig. 9** Microstructures after deformation at  $T = 1273$  K,  $\dot{\epsilon} = 0.01$  s $^{-1}$ ,  $\epsilon = 0.45$  and hold for **a** 0 s and **b** 60 s

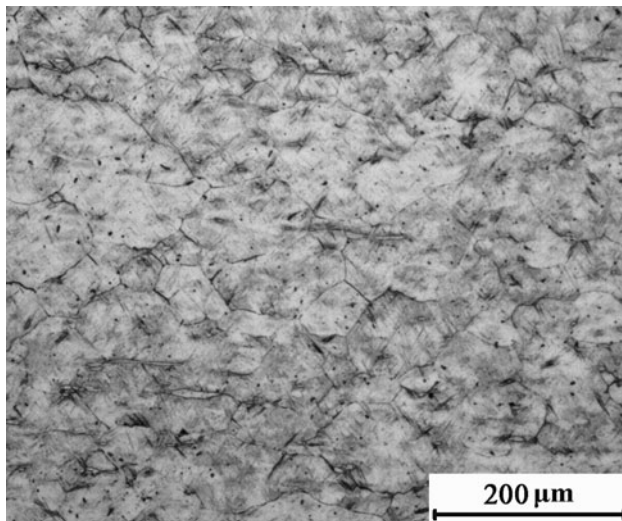


**Fig. 10** Microstructure after the interrupted test at  $T = 1273$  K,  $\dot{\varepsilon} = 0.01 \text{ s}^{-1}$ ,  $t_{\text{int}} = 100$  s

fraction of equiaxed grains (Fig. 10). This indicates that recrystallization was sped up in the second deformation. Similar behavior has been reported for multistage deformation of an OFHC copper by Kugler et al. [28]. The steady state flow stress, however, is not affected by the initial grain size, which is consistent with the reported DRX behavior.

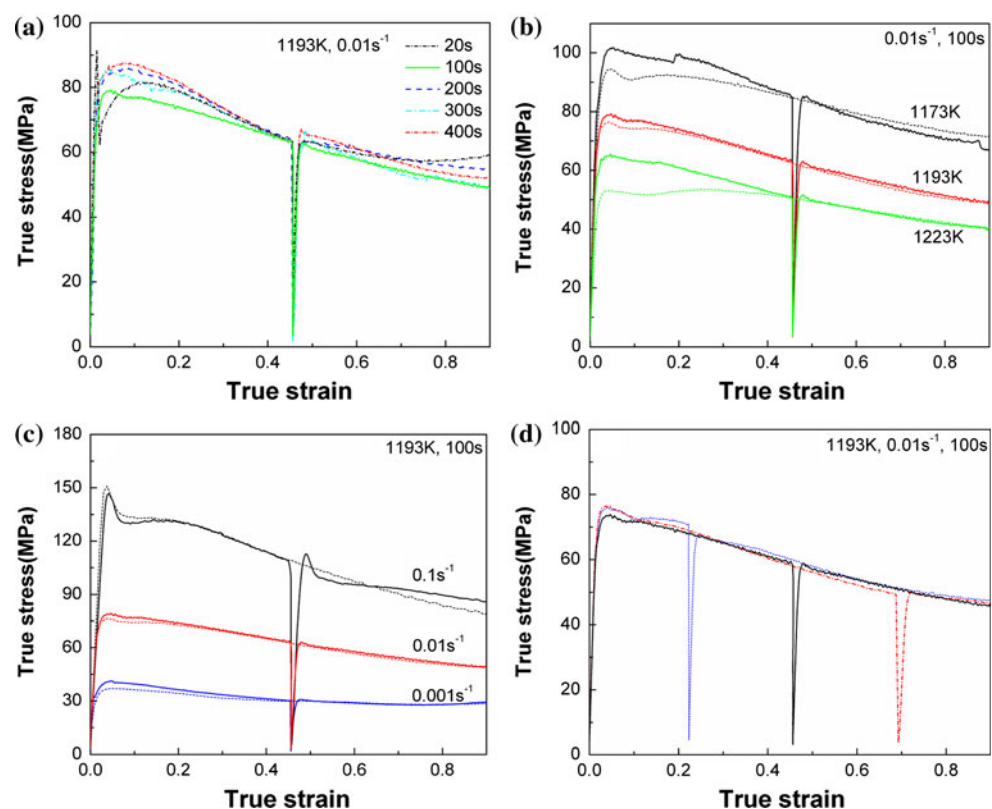
### Multistage ( $\alpha + \beta$ ) working

**Multistage flow stress behavior** In multistage deformation, the processing parameters, such as working temperature, strain rate, holding time, and interruption strain, have strong influence on the restoration behavior during interruption and affect the following deformation behavior and microstructure development.

Figure 11a shows the flow stress curves at 1193 K and  $0.01 \text{ s}^{-1}$  under different inter-pass times. The flow stress curves also show low peak strains and strong flow softening in the second deformation. The measured 0.2% yield stress ( $\sigma_{0.2,II}$ ) upon reloading varied little with holding time and was smaller than the yield stress in the first deformation ( $\sigma_{0.2,I}$ ). This is different from what is commonly observed during the interrupted hot deformation of other metals whereby the yield stress decreases with inter-pass holding [7]. The phenomenon that the yield stress up reloading displays no discernible relationship with holding time has been observed in the Mg–3Al–1Zn magnesium alloy [7] and IMI834 titanium alloy [1]. These alloys also exhibit a similar flow stress behavior of low peak strain and significant flow softening upon reloading, which is different from other metals, e.g., steel [4].

The peak stress upon reloading ( $\sigma_{p,II}$ ) was very close to the flow stress prior to interruption ( $\sigma_{\text{int}}$ ) at time intervals

**Fig. 11** Interrupted stress–strain curves under different working conditions



up to 200 s and then increased with inter-pass time. The investigations on Mg–3Al–1Zn [7] and IMI834 [1] suggested that the peak stress upon reloading is associated with softening fraction. The peak stress increases with softening fraction. Therefore, SRX may be the main softening mechanism during inter-pass holding.

Figure 11b illustrates the interrupted stress–strain curves at temperatures below the  $\beta$  transus. The peak stress upon reloading is close to the flow stress prior to interruption at all testing temperature, though the holding time is comparable to the deformation time. As a result, the interrupted flow stress curve converges to the corresponding uninterrupted curve immediately after the peak stress. The interrupted stress–strain curves at different strain rates and a temperature of 1193 K are shown in Fig. 11c. Though the holding time was of one order longer than the deformation time at a strain rate of  $0.1 \text{ s}^{-1}$ , the peak stress in the second deformation was a little larger than the flow stress prior to interruption. It is confirmed that SRX dominated the softening in a wide range of temperatures and strain rates. Figure 11d illustrates the flow stress curves interrupted at different strains. It is found that  $\sigma_{p,II}/\sigma_{int}$  increases slightly with interruption strain. This is because the increase of microstructure inhomogeneity with strain promoted the SRX process during interruption thus increased the softening fraction. Lin et al. [4] also observed that the MDRX kinetics of 42CrMo steel increases with deformation degree.

**SRX kinetics** The offset method is commonly used to evaluate the softening caused by MDRX and recovery, in which the softening fraction  $X$  is calculated by:

$$X = \frac{\sigma_{int} - \sigma_{0.2,II}}{\sigma_{int} - \sigma_{0.2,I}} \quad (3)$$

Equation 3 cannot be applied in this study as  $\sigma_{0.2,II}$  varied little with holding time. Other methods [29], such as 2% offset, back extrapolation, 5% total strain and mean flow stress methods, are not suitable in this paper, either.

For materials exhibiting a deformation behavior similar to TA15 alloy, it has been found that the peak stress is a proper index to softening [1, 7]. Vo et al. [1] proposed the following equation to measure the softening fraction:

$$X = \frac{\sigma_{p,II} - \sigma_{int}}{\sigma_{p,I} - \sigma_{int}} \quad (4)$$

The calculated softening fraction using Eq. 4 is given in Fig. 12. The softening rate increased with temperature and strain rate. For both single phase and two phase alloys, the SRX/MDRX kinetics increases with strain rate, as high deformation rate suppresses the restoration process, yields high stored energy and consequently provides large driving force for recrystallization. However, the variation of

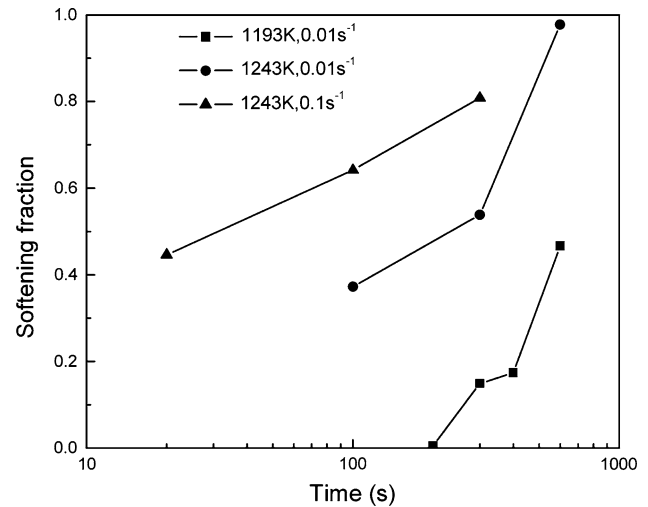


Fig. 12 Softening fraction as a function of holding time

SRX/MDRX kinetics with temperature in two phase alloys may be quite different from that in single phase alloys. Post deformation recrystallization is governed by two processes: nucleation and growth of recrystallizing grains. Nucleation and grain growth are thermally activated processes. Therefore, recrystallization kinetics increases with temperature in single phase alloys. For two phase alloys, the existence of second phase may affect the nucleation and growth of recrystallizing grains in the matrix. Vo et al. [1] found that the IMI834 alloy with an initially bimodal microstructure displays more rapid post deformation recrystallization rate with decreasing temperature and attributed it to the increase in  $\alpha$  phase fraction which refines the initial  $\beta$  grain, increases the deformation inhomogeneity, and thereby provides more nucleation sites. In current study, however, the recrystallization rate increases with temperature in subtransus working. Though high deformation temperature may reduce the nucleation rate, it increases the grain boundary mobility [30] and reduces the drag force of second phases on the matrix grain boundaries [31]. The boundary migration rate increases with temperature. Consequently, the post deformation recrystallization is accelerated at high temperatures.

**Microstructure evolution** Figure 13 illustrates the microstructure of the specimens deformed to the interrupted strain and held for different times. The  $\alpha_p$  were slightly elongated transverse to the compression axis. No obvious break-up of  $\alpha_p$  were observed at all holding times. During annealing of deformed titanium alloys with initially lamellar structure, the break-up of lamellar  $\alpha$  is commonly observed. It has been found that the break-up of lamellar  $\alpha$  is characterized by segmentation of  $\alpha$  lamellae by processes such as boundary splitting and edge spheroidization [32]. The recovery-induced dislocation substructure in  $\alpha$  phases



plays an important role in boundary splitting. In this study, the strain imposed on  $\alpha_p$  was small, not only because the total strain was small but also because strain partitioning between  $\alpha_p$  and  $\beta$  matrix occurred. The driving force for boundary splitting might be insufficient. As a result, the  $\alpha_p$  break-up was not significant. Another mechanism accounting for the globularization of  $\alpha$  phases is the microstructural coarsening driven by the reduction in interface energy [32]. However, static coarsening is not significant unless prolonged annealing [32, 33]. In this study, the holding time was not long enough for coarsening induced globularization. As a result, the aspect ratio and grain size of  $\alpha_p$  varied little with holding time under the conditions of current experiments.

There existed a large fraction of pancaked  $\beta$  grains after holding for 300 s. With increasing holding time, a lot of equiaxed  $\beta$  grains appeared. The microstructure observation also suggested that SRX of the  $\beta$  phases took place during isothermal holding. The average aspect ratio of  $\beta$

phases decreased as SRX proceeded. The average grain size decreased slightly, too. Figure 13b shows the microstructure after isothermal holding for 600 s. Though the interrupted flow stress curve suggested that full recrystallization was achieved (Fig. 12), a small fraction of pancaked  $\beta$  grains were observed between the intervals of elongated  $\alpha$  grains. It indicates that the morphology of the  $\alpha_p$  influences that of the  $\beta$  grains.

Figure 14 shows the microstructure after reloading. The  $\alpha_p$  were further pancaked in the second deformation. The break-up of  $\alpha_p$  was minor though additional deformation, as the  $\alpha_p$  aspect ratio increased slightly. The average  $\beta$  grain size and aspect ratio varied little regardless of inter-pass holding time. It has been found in the single phase materials that the dynamic recrystallized grain size is not influenced by the initial grain size [27]. Though the isothermal holding affected the  $\beta$  grain size prior to the second deformation, it did not influence the final grain size.

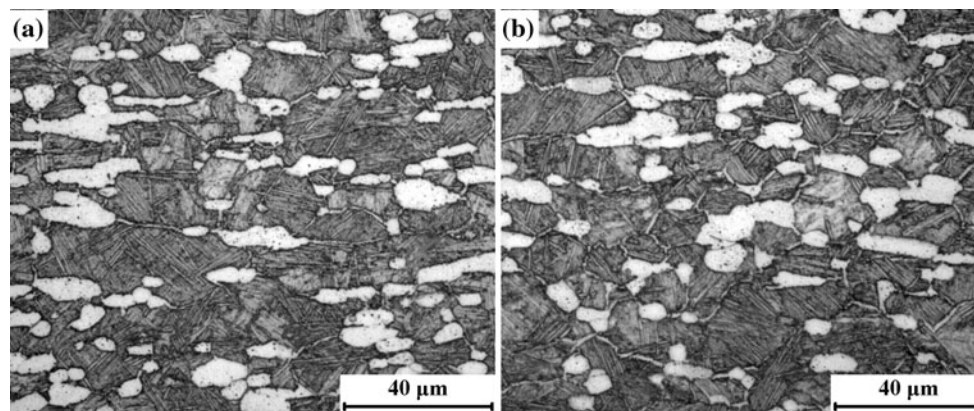


**Fig. 13** Microstructure after deformation at  $T = 1273$  K,  $\dot{\epsilon} = 0.01$  s $^{-1}$ ,  $\epsilon = 0.45$  and hold for **a** 300 s and **b** 600 s. The compression axis is vertical

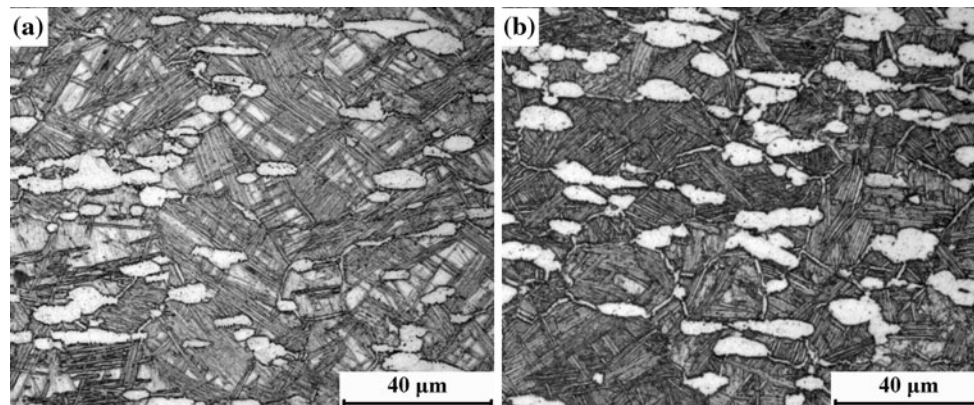


**Fig. 14** Microstructure after interrupted tests at a temperature of 1243 K, strain rate of  $0.01$  s $^{-1}$  and holding times of **a** 300 s and **b** 600 s. The compression axis is vertical

Previous investigation [34] also suggests that the dynamic recrystallized grain size is only a function of Zener–Hollomon parameter,  $Z = \dot{\epsilon} \exp(Q/RT)$ . It decreases with increasing Zener–Hollomon parameter (i.e., a higher strain rate or a lower temperature). In this study, it is found that the recrystallized  $\beta$  grain size is more affected by the working temperature but less dependent on the strain rate, as shown in Fig. 15. The  $\beta$  grain size increased sharply with temperature but varied little with strain rate at a certain working temperature. It can be seen that the  $\beta$  grain size is determined by the spacing of the  $\alpha_p$ , which is greatly influenced by the working temperature. Therefore, the  $\beta$  grain size is not related to the Zener–Hollomon parameter, as given in Fig. 16.

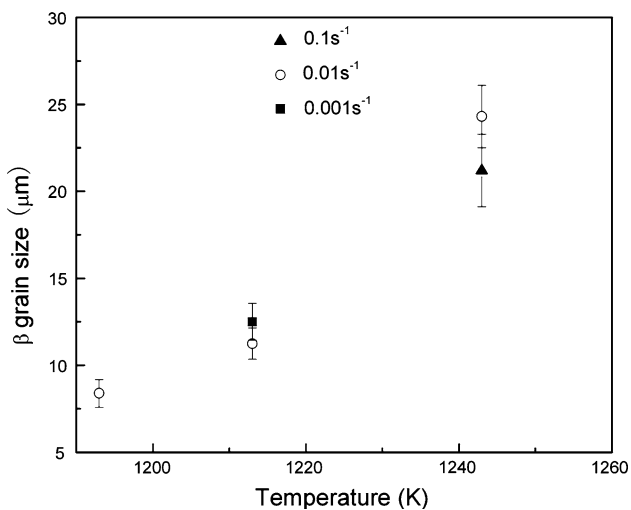


**Fig. 15** Measured  $\beta$  grain size after interrupted test at different working conditions

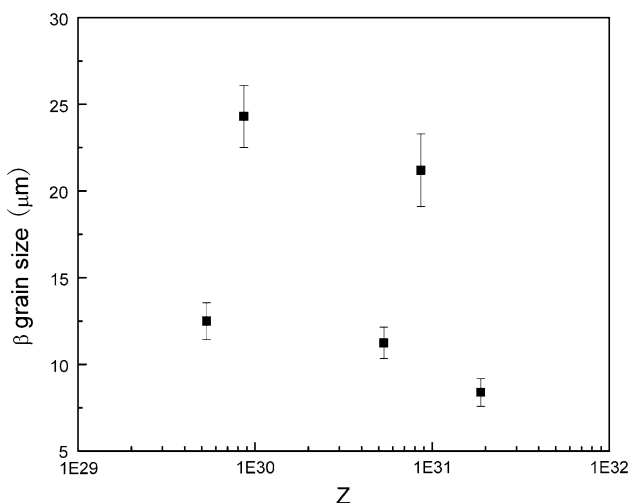


**Fig. 16** Plot of  $\beta$  grain size versus Zener–Hollomon parameter

## Conclusions

The deformation behavior and microstructure evolution of TA15 titanium alloy under multistage deformation have been investigated in the temperature range of 1173–1273 K, strain rate range of 0.001–0.1  $s^{-1}$  by interrupted compression tests. From this work, the following conclusions were drawn:

- (1) The TA15 titanium alloy exhibits significant flow softening in both  $\beta$  and  $\alpha + \beta$  working. The flow softening relates to dynamic recrystallization of  $\beta$  phases. The recrystallization kinetics decreases with strain rate in  $\beta$  phase field, which is similar to the materials with low-to-medium stack fault energy.
- (2) Metadynamic recrystallization is the main softening mechanism during inter-pass holding of multistage  $\beta$  working. The grain refinement by metadynamic recrystallization leads to the decrease in peak stress upon reloading.
- (3) In multistage  $\alpha + \beta$  working, the flow stress curves show low peak strain and strong flow softening upon reloading. Static recrystallization is the main softening mechanism during inter-pass holding. The static recrystallization kinetics increases with temperature and strain rate.
- (4) In multistage  $\alpha + \beta$  working, the inter-pass holding has little influence on the morphology of the primary  $\alpha$  phases. The  $\beta$  grain size is determined by spacing of primary  $\alpha$  phases, which is more affected by working temperature but less dependent on strain rate and inter-pass holding time.

**Acknowledgements** The authors would like to gratefully acknowledge the support of Natural Science Foundation for Key Program of China (No. 50935007) and National Basic Research Program of China (No. 2010CB731701).

## References

1. Vo P, Jahazi M, Yue S (2008) Metall Mater Trans A 39:2965
2. Liu Y, Zhu J, Wang Y, Zhan J (2008) Mater Sci Eng A 490:113
3. Sun ZC, Yang H, Han GJ, Fan XG (2010) Mater Sci Eng A 527:3464
4. Lin YC, Chen MS, Zhong J (2009) J Mater Process Technol 209:2477
5. Lin YC, Chen MS (2009) Mater Sci Eng A 501:229
6. Weaver DS, Semiatin SL (2007) Scripta Mater 57:1044
7. Beer AG, Barnett MR (2009) Scripta Mater 61:1097
8. Sheppard T, Norley J (1988) Mater Sci Technol 4:903
9. Ding R, Guo ZX (2004) Mater Sci Eng A 365:172
10. Ma F, Lu W, Qin J, Zhang D (2006) Mater Sci Eng A 416:59
11. Jackson M, Dashwood R, Christodoulou L, Flower H (2005) Metall Mater Trans A 36:1317
12. Zong YY, Shan DB, Xu M, Lv Y (2009) J Mater Process Technol 209:1988.

13. Zong YY, Shan DB, Lu Y (2006) *J Mater Sci* 41:3753. doi: [10.1007/s10853-006-2658-z](https://doi.org/10.1007/s10853-006-2658-z)
14. Wanjara P, Jahazi M, Monajati H, Yue S, Immarigeon JP (2005) *Mater Sci Eng A* 396:50
15. Huang LJ, Geng L, Li AB, Cui XP, Li HZ, Wang GS (2009) *Mater Sci Eng A* 505:136
16. Furuhashi T, Poorganji B, Abe H, Maki T (2007) *JOM* 59:64
17. Ding R, Guo ZX, Wilson A (2002) *Mater Sci Eng A* 327:233
18. Semiatin SL, Montheillet F, Shen G, Jonas JJ (2002) *Metall Mater Trans A* 33:2719
19. Vo P, Jahazi M, Yue S, Bocher P (2007) *Mater Sci Eng A* 447:99
20. Weiss I, Semiatin SL (1999) *Mater Sci Eng A* 263:243
21. Luo J, Li M, Li H, Yu W (2009) *Mater Sci Eng A* 505:88
22. Niu Y, Hou H, Li M, Li Z (2008) *Mater Sci Eng A* 492:24
23. Momeni A, Abbasi SM (2010) *Mater Design* 31:3599
24. Li MQ, Pan HS, Lin YY, Luo J (2007) *J Mater Process Technol* 183:71
25. Briottet L, Jonas JJ, Montheillet F (1996) *Acta Mater* 44:1665
26. Philippart I, Rack HJ (1998) *Mater Sci Eng A* 243:196
27. Blaz L, Sakai T, Jonas JJ (1983) *Metal Sci* 17:609
28. Kugluer G, Turk R (2004) *Acta Mater* 52:4659
29. Fernández AI, López B, Rodríguez-Ibabe JM (1999) *Scripta Mater* 40:543
30. Hunphreys FJ, Hatherly M (2004) *Recrystallization and related annealing phenomena*, 2nd edn. Pergamon Press, Oxford
31. Nes E, Ryum N, Hunderi O (1985) *Acta Metall* 33:11
32. Stefansson N, Semiatin SL (2003) *Metall Mater Trans A* 34:691
33. Semiatin SL, Kirby BC, Salishchev GA (2004) *Metall Mater Trans A* 35:2809
34. Sakai T, Jonas JJ (1984) *Acta Metall* 32:189